International Journal of Computer (IJC)

ISSN 2307-4523 (Print & Online)

http://ijcjournal.org/

Elaboration of Processing Chains for Spatio-temporal Analysis of Rainfall Data Application: Alaotra Mangoro Region, Madagascar

Aimé Richard Hajalalaina[a*], Arisetra Razafinimaro[b], Niry Arinavalona Rakotovao[c], Adolphe Ratiarison[d]

[a,b]*School of management and Technological Innovation, Fianarantsoa University,Fianarantsoa BP 1135, Madagascar*

[a,b]*Laboratory of Computer Science and Mathematics Applied to Development, Fianarantsoa University,Fianarantsoa, Madagascar*

[a,b]*Informatics-Geomatics Mathematics and Applications, Fianarantsoa University, Fianarantsoa, Madagascar*

[c,d]*Laboratory of Dynamics of the Athmosphere, Climate and Oceans, Antananarivo University, Madagascar*

[a]*Email: arhajalalaina@yahoo.fr*

Abstract

This present study was carried out within the framework of the automation of the processing chains of spatio-temporal data processing of climatological data in Madagascar. Our objective is to develop and automate the processing chains of rainfall data from ERA-Interim re-analyses of the European Meteorological Centre ECMWF to observe and analyze the evolution of precipitation over time and space. The chains are elaborated in a generic way by introducing statistical methods such as spatial interpolation, calculation of temporal and spatial averages, maximum entropy method, and principal component analysis. Then, the elaborated chains are implemented with MATLAB. Thus, the test of these chains has been performed in the Alaotra Mangoro region. The results obtained allowed us to observe, analyze and interpret the evolution of precipitation in this region of Madagascar during 35 years (1979 to 2013).

Keywords: treatment chain; reanalysis; spatio-temporal analysis; precipitation; Madagascar.

----

* Corresponding author.

1. Introduction

Nowadays, climate change has been a topic of concern not only to scientists but also to every organization working in different fields. Indeed, all human activities depend on climate variation whatever their field of activity, which makes the importance of the role of climate on the economy and human life. Geographically, located between the equator and the Tropic of Capricorn, Madagascar generally enjoys a so-called tropical climate. Rainfall plays a very important role on the economic activity of Malagasy people. Indeed, Madagascar's economy is based on agriculture with the agricultural sector contributing about 30% of the Gross Domestic Product (GDP), an economic indicator used to measure production in a given country, and 80.4% of the population works in the agricultural sector [1]. It is for these multiple reasons that we have chosen the Alaotra Mangoro region as the study area for rainfall analysis. Indeed, this region is the first rice granary in Madagascar. Rice remains the main strategic crop and the staple food of the Malagasy population. We are now witnessing a climatic disturbance in this region that could damage rice production. The objective of our study is to elaborate and automate process chain of reanalysis rainfall data to analyze rainfall which is a predominant climatic parameter in this region in order to adapt to climate change. The main thrusts of our studies focus on temporal and spatial analysis of precipitation data. The impact of climate change in the Malagasy countryside deserves to be underlined because the activities of the peasant are still strongly dependent on climate and more particularly on precipitation. The effects on the economy are notorious: the lack of water results in drought and therefore a drop in production. The surplus of water leads to flooding and consequently to a drop in production [2]. Given the technological evolution of the sensors on board meteorological satellites, the potential of satellite data is increasing in such a way that the question now arises of how to exploit it as efficiently as possible. New climatological data will be accessible from day to day. It is for these reasons that we propose automatic processing chains for rainfall data from these observation devices. These chains will be developed to assist climatologists to capitalize on their knowledge in order to analyze and observe existing rainfall phenomena.

2. Study area

We chose the Alaotra Mangoro region as the study area. It covers an area of 33054 km². It has a large cultivable area and all speculations in agriculture are possible. The extent of the areas allows the establishment of large farms to grow crops.

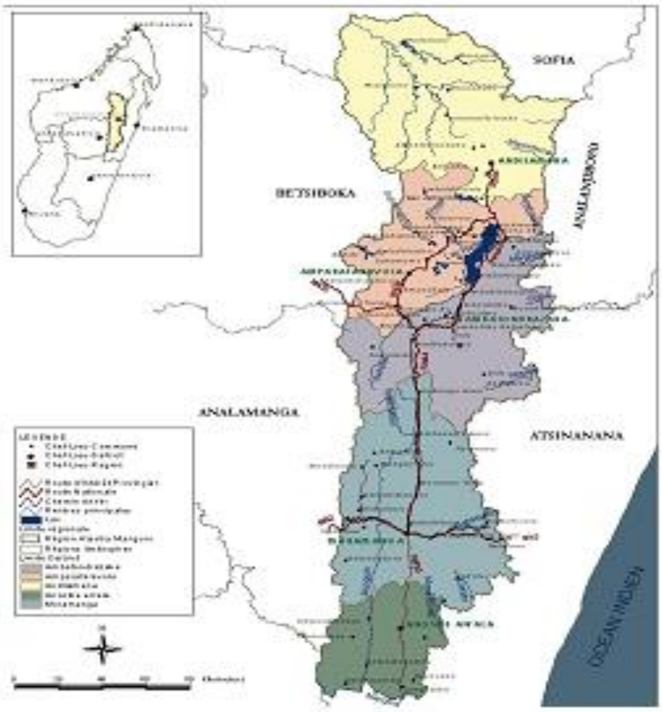

Figure 1: Map of the Alaotra Mangoro region (sources: FTM BD 500 - Realisation: UGI Alaotra Mangoro, June 2005)

Geographically, this region is located between longitudes 47°E and 49°E, and latitudes 20°S latitudes 16°S. It is bounded to the north by the Sofia region (Mandritsara District); to the northwest by the Betsiboka region (Tsaratanàna District); to the west by the Analamanga region (Anjozorobe and Manjakandriana Districts); to the south by the Atsinanana region (Marolambo District); to the southwest by the Vakinankaratra region; to the east by the Atsinanana and Analanjirofo regions. It is administratively constituted by five (5) districts (Andilamena, Amparafaravola, Ambatondrazaka, Moramanga and Anosibe An'Ala). The reason for the choice of this region is that it is the first rice granary in Madagascar. Rice remains the main strategic crop and the staple food of the Malagasy population. Disruption due to climate change could damage the agricultural system in general and rice production in particular in the region mentioned above. One of the most important climatic variables is rainfall. It is one of the necessary conditions for rice cultivation. Changes have been observed in the quantity, shortening of the period and delay of rainfall in this region due to climate change. As a result, several hectares of rice fields are experiencing a remarkable lack of water, leading to a disruption of the cropping calendar (a delay in tillage, and a shortening of the cropping season in general), a decrease in cultivated area and a drop in production [3,4]. In order to address these problems, we need an efficient and rapid tool that will allow us to analyze rainfall in this area using temporal and spatial analysis methods.

3. Data, methods and tools

3.1. Data

The precipitation data that we will process are obtained free of charge, by download from the European Center for Medium-range Weather Forecast (ECMWF) website. These data are raw data in NETCDF format, with a spatial resolution of 1°x1°. They are called reanalysis data. These data have been collected on a daily basis and have a three-dimensional raster structure (latitudes, longitudes, days). They are geolocalized using the WGS84 geographic reference system (World Geodesic System of 1984). Other climatological data with the same characteristics are provided in the same format by the NOOA, METEOSAT, ERS, ENVISAT and METEOSAT Second Generation satellites and others are also available from the Malagasy General Directorate of Meteorology. Vector data administratively limiting the study area were obtained from the FTM (Foibe Taontsaritan'i Madagasikara), the national geographical institute of Madagascar, which deals with cartography and provides geographical data of Madagascar.

3.2. Methods

Our method is based on a computer vision of the conceptualization of processing chains dedicated to the study and spatio-temporal analysis of rainfall data. To do so, we propose a generic processing chain for rainfall data that includes three main steps. The first concerns the pre-processing of raw reanalysis data, the processing of temporal analyses and the processing of spatial analyses. These three steps are described below. A processing chain is a sequence of treatments that receive data as input and produce output results for analysis. Experts in the field then intervene to exploit and interpret these results in order to draw conclusions. We propose a method based on the use of a generic processing chain to analyze the rainfall data from the various sources mentioned above in order to produce data that can be used for rainfall studies. Figure 2 shows the proposed processing chain using raw data, pre-processing data, spatial and temporal analysis data. On the other hand, the same chain is composed of composite treatments including pre-treatments, temporal and spatial analysis treatments.

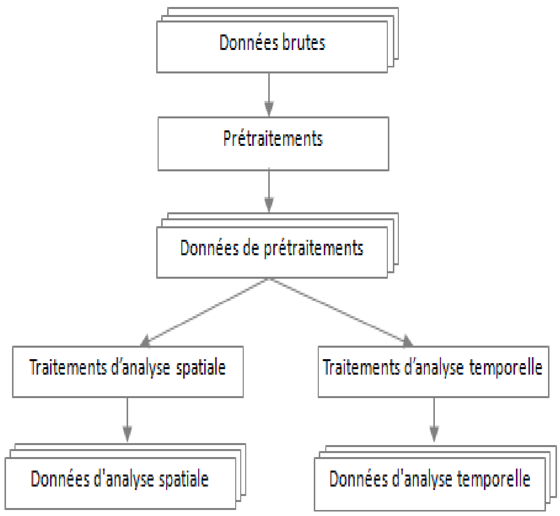

Figure 2: Generic Rainfall Data Processing Chain

The raw reanalysis data from the different sources undergo different levels of pre-processing to transform them into intermediate data. These will be commonly used, as input parameters, for the final processing of spatial and temporal precipitation analyses. The results of these two treatments produce respectively the spatial and temporal analysis data.

Step 1: Pre-processing of rainfall data

Not all the data from reanalyses are immediately usable, which we call "raw data", they have to undergo a certain amount of pre-processing. We propose a processing chain, shown in Figure 2, the different steps required for raw reanalysis data. The rainfall data pre-processing chain we propose receives the raw data that undergoes the "raw data processing". These treatments start with the loading of the source data files, followed by the correction of measurement errors or the restitution of missing data and the unit conversion if necessary. Then, we proceed to the "extraction of the areas of interest" on the obtained "processed raw data". This processing results in "Areas of interest data" which will be interpolated at a resolution more or less high depending on the size of the chosen area. If the area of interest is large enough, i.e. at the national or inter-regional level, a high resolution of 0.5°x0.5 is sufficient. If the area is small, i.e. at the regional level, a resolution of 0.25°x0.25° or 0.1°x0.1° will be chosen. The final results of this treatment are the "Interpolated Data".

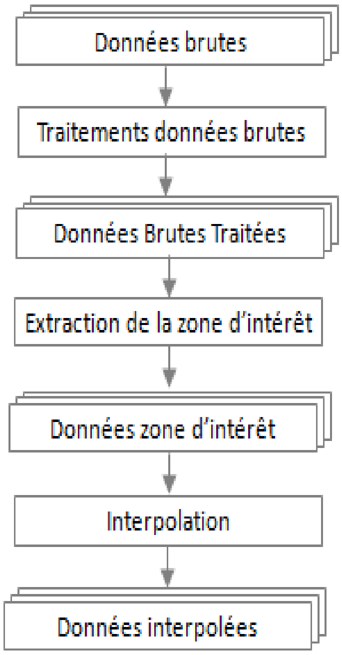

Figure 3: Rainfall data pre-processing chain

Step 2: Temporal analysis of rainfall data

For the temporal study of precipitation reanalysis data, we propose the processing chain shown in Figure 4. This chain takes as input the "interpolated data", results of the pre-processing chain, which serve as input parameter for the two treatments, the "statistical treatments" and "spectral treatments" giving results to the "temporal analysis data". The temporal statistical treatments can group statistical methods applied to rainfall data to study central tendency parameters [5], such as daily, monthly and annual climatological averages, daily, monthly and annual totals. For treatments in spectral analysis, several methods can be applied such as anomaly calculation, maximum entropy method [6,7,8] and filtering [9]. The results of this processing chain are generally analysis curves or qualitative data describing the temporal variability of rainfall.

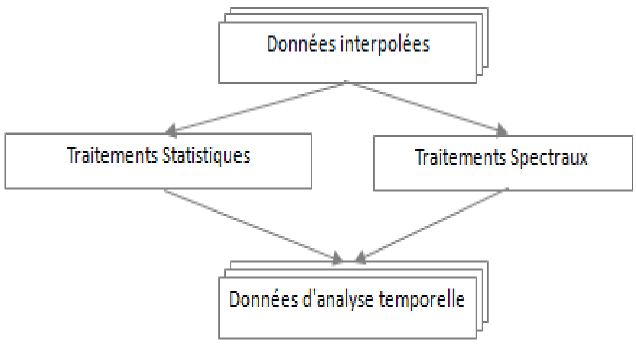

Figure 4: Processing chain for temporal analysis of rainfall data

Step 3: Spatial analysis of rainfall data

For the spatial study of rainfall data, we propose the processing chain shown in Figure 5. This chain takes as input the "interpolated data", results of the pre-processing chain, and the vector layer corresponding to the area of interest. The two data will be integrated into one using the geometric intersection operation (taking into account the coordinate system used) for geolocalized data. This processing results in a "rainfall map", which will be analyzed by applying the statistical treatments. Many treatments are applicable to the spatial analysis of rainfall data, among them the spatial distribution of rainfall (monthly, annual, decennial), the spatial distribution of the number of rainy days and the principal component analysis [10,11,12,14]. The results of this processing chain can be thematic maps or qualitative data describing the spatial distribution of rainfall.

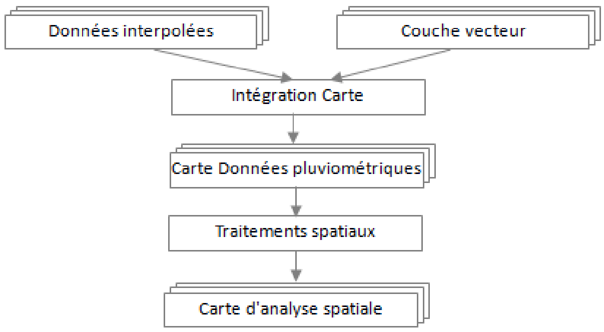

Figure 5: Spatial Rainfall Data Analysis Processing Chain

3.3. Tools

We used MATLAB (Matrix laboratory) software to implement the rainfall data processing chains we had previously designed. MATLAB is a very powerful scientific computational programming language. Developed by The MathWorks company, it allows you to manipulate matrices, display curves, maps and data, and implement numerical calculation algorithms .MATLAB users, about one million in 2004 [14], come from a wide variety of backgrounds, including engineering, science, and economics in both industrial and research settings. We bring our particular intention in the field of climatology to the case of the DyACO laboratory. MATLAB can be used alone or with dozens of toolboxes. Among them, we are interested in the statistic toolbox

[15], Signal processing toolbox [16] and Mapping toolbox [17]. These toolboxes are used to implement our methodology based on the temporal and spatial rainfall analysis processing chains in order to produce curves and maps for observation.

4. Results

4.1. Temporal analysis of rainfall over the period 1979 to 2013

4.1.1. Annual rainfall analysis

Figure 6 below shows the curve of average annual rainfall over the period from 1979 to 2013.

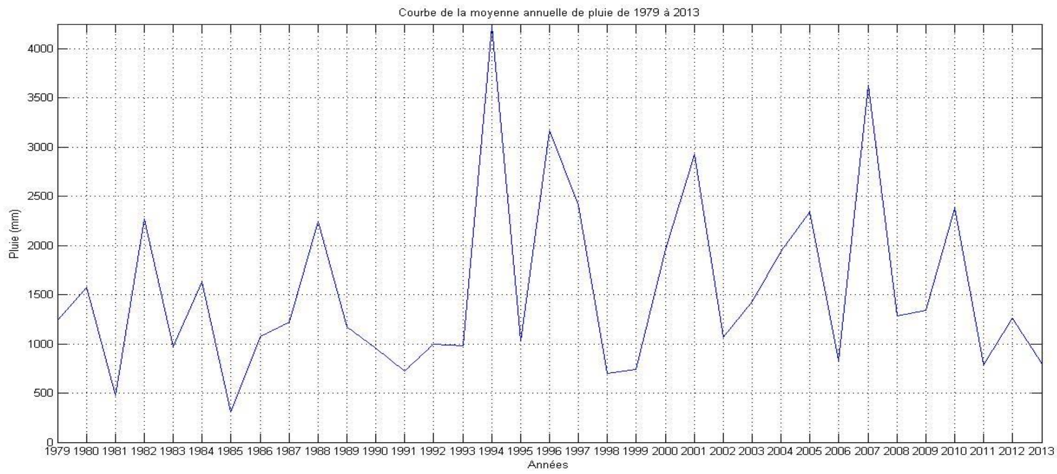

Figure 6: Curve of Average Annual Rainfall from 1979 to 2013

Analyzing the curve in Figure 6, we observe that the amount of rainfall reaches its highest level in 1994 with a height of more than 4000 mm. The lowest level is observed in 2013 with a height of 850 mm. We also observe that rainfall amounts in the Alaotra Mangoro region have decreased over the last four years. Figure 7 shows the cumulative annual rainfall for 35 years. This accumulation shows us an ascending curve, but from the year 1993 we observe an irregularity because from that year on, a slight upward flexibility is observed in the curve until 1997. This change coincides with the significant increase in the amount of rainfall between 1993 and 1997 observed in the analysis of the average annual rainfall shown in Figure 6. But from the year 2011 onwards, we see another irregularity in the annual rainfall accumulation that there is a slight downward flexibility. This coincides with the decrease in the amount of rainfall, between 2010 and 2013, observed on the annual average rainfall curve in Figure 6. This shows us that there has been a decrease in the amount of rainfall each year for the last three years. This explains the dryness of a few hectares of rice fields, which has led to the decrease in rice production in the Alaotra Mangoro region.

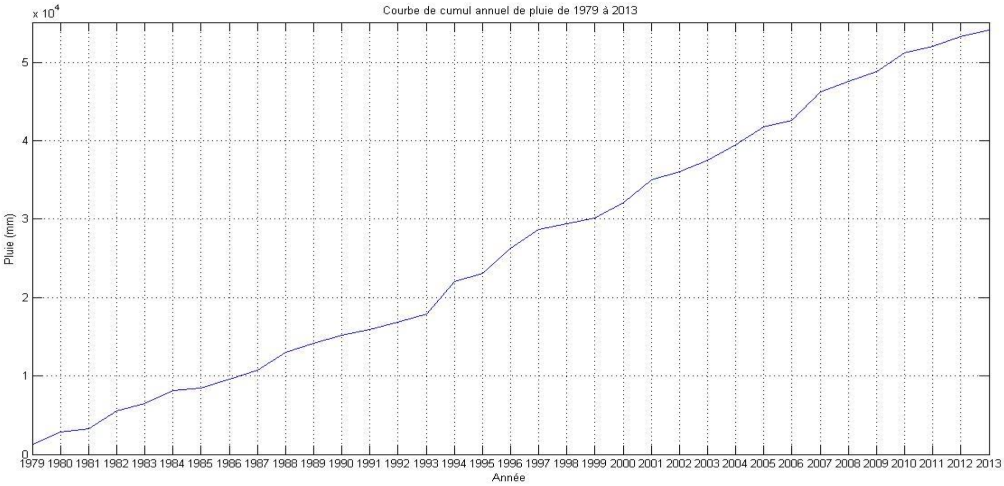

Figure 7: Annual Rainfall Cumulative Curve from 1979 to 2013

4.1.2. Monthly Rainfall Analysis

The monthly variation in rainfall in the Alaotra Mangoro region over 35 years (from 1979 to 2013) is given by the monthly climatological average represented in Figure 8.To calculate the monthly climatological average, monthly averages were collected for each year, i.e. each month of the year has its average amount of rainfall. Then the average rainfall amounts for the same month, such as every January month from 1979 to 2013, were averaged over the 35 years from 1979 to 2013.

Two major differences are observed during one year :

A phenomenon with monthly rainfall intensities less than or equal to 1.3 mm between the months of June and November. This phenomenon is known as the dry and cool season (or winter) in general in Madagascar. A phenomenon with monthly rainfall intensity greater than 1.3 mm, between the months of December and May. This phenomenon is known as under the name of the rainy season (or summer) in general in Madagascar.

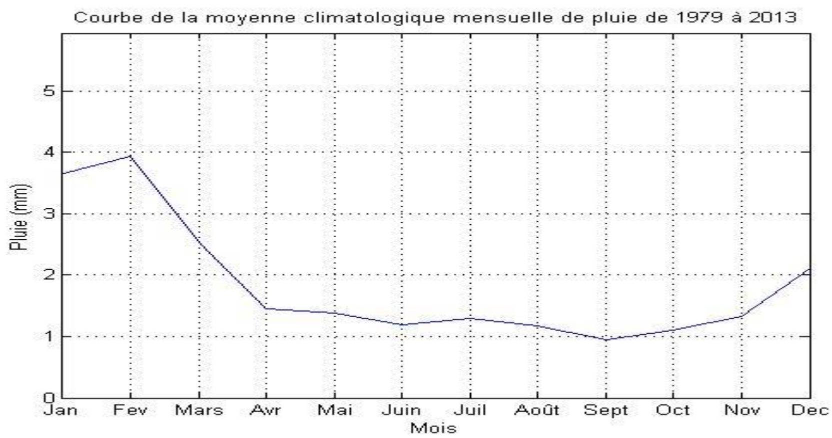

Figure 8: Curve of monthly climatological mean rainfall from 1979 to 2013

A slight increase is noted in July during the winter. This explains the presence of a moderately significant rainfall event during the winter in the Alaotra Mangoro region from 1979 to 2013.

4.1.3. Daily Rainfall Analysis

The daily rainfall, shown in Figure 9, is the amount of gross daily rainfall for 35 years. It is calculated from the amount of rain per day from January 1, 1979 to December 31, 2013.

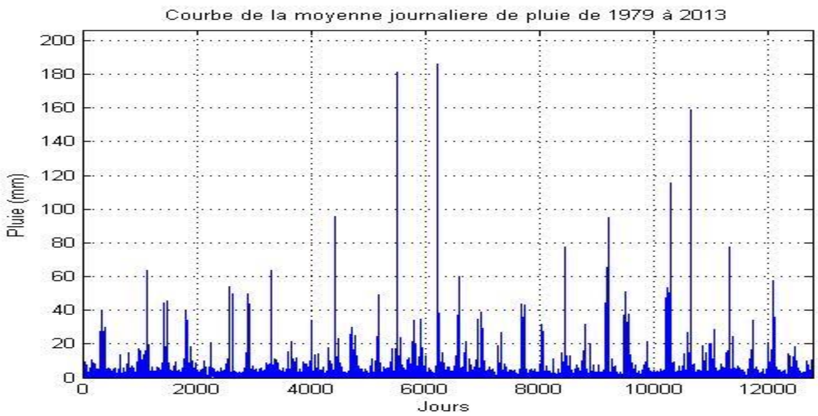

Figure 9: Curve of average daily rainfall from 1979 to 2013

We notice a pseudo-periodicity of rain during 35 years of observations. With the exception of the year 1998 when the rainfall reached 187mm. The lowest is observed in 2013 which reaches the minimum level of 0 mm. The daily rainfall variation in the Alaotra Mangoro region for 35 years (from 1979 to 2013) is given by the daily climatological mean represented in Figure 10. Indeed, to calculate the daily climatological average, daily averages were collected for each year, i.e. each day of the year has its average amount of rainfall. Then, the average rainfall amounts for a single day, such as all the first days of January from 1979 to 2013, were averaged over the 35 years from 1979 to 2013.

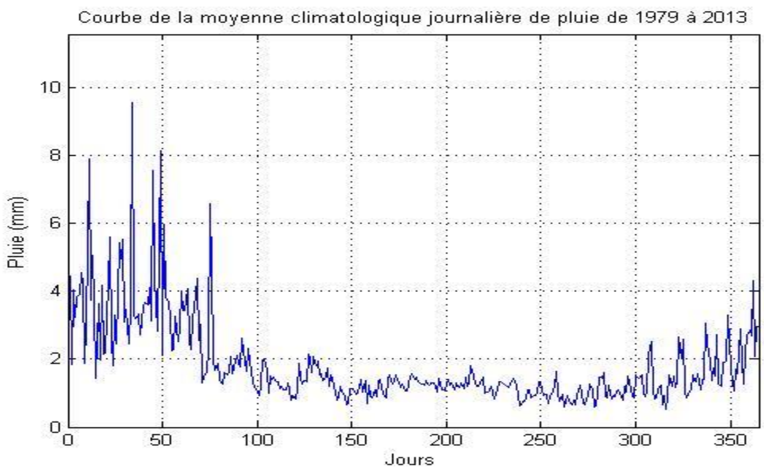

Figure 10: Curve of the daily climatological mean rainfall from 1979 to 2013

Figure 10 also shows us what we have just said above. It is significant during the period from December to May and is minimal during the period from June to November. During 35 years, from 1979 to 2013, the rainfall is maximum at the beginning of February with a value of 9.4 mm and it is minimum in September with a value of 0.7 mm. The cumulative daily rainfall is given in Figure 11. This cumulative rainfall over 35 years in the Alaotra Mangoro region shows us regularly rising curves. This shows that there has been no significant change in daily rainfall for 35 years.

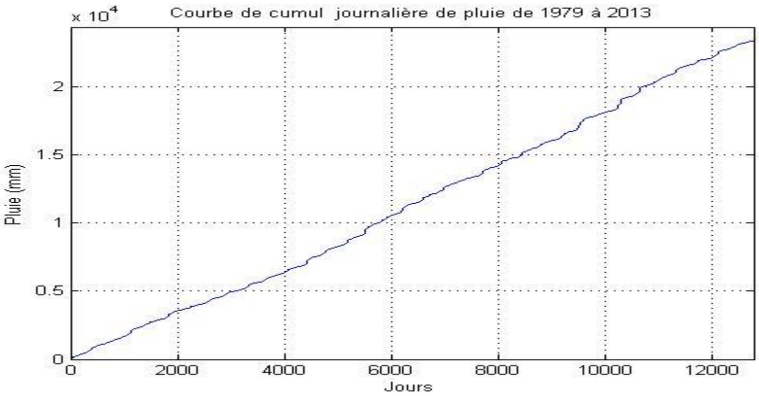

Figure 11: Daily Rainfall Cumulative Curve from 1979 to 2013

4.1.4. Spectral Analysis of Rainfall by the Maximum Entropy Method

Applying the maximum entropy method, we obtain Figure 12.

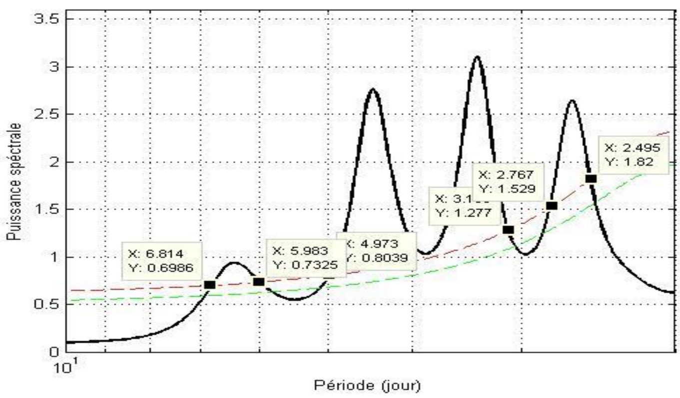

Figure 12: Spectral Power Curve of the Anomaly and the Rain MEM from 1979 to 2013

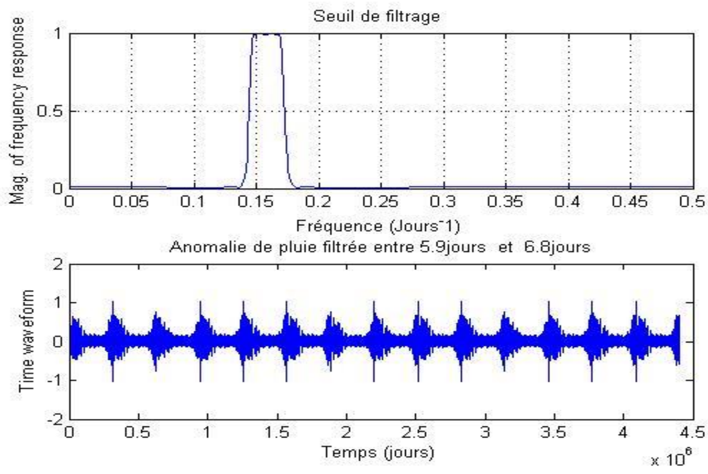

Figure 13: Filtering threshold and daily anomaly curves for filtered data between 5.9 days and 6.8 days

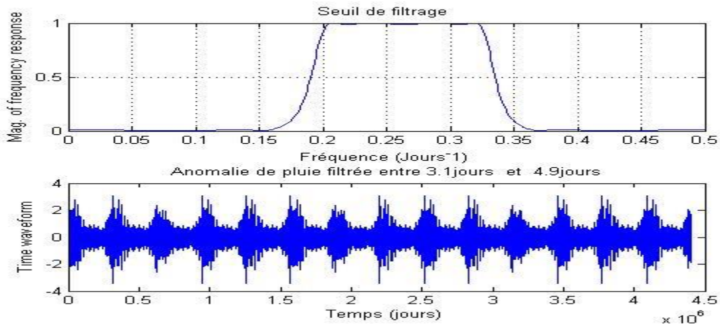

Figure 14: Filtering threshold and daily anomaly curves for filtered data between 3.1 days and 4.9 days

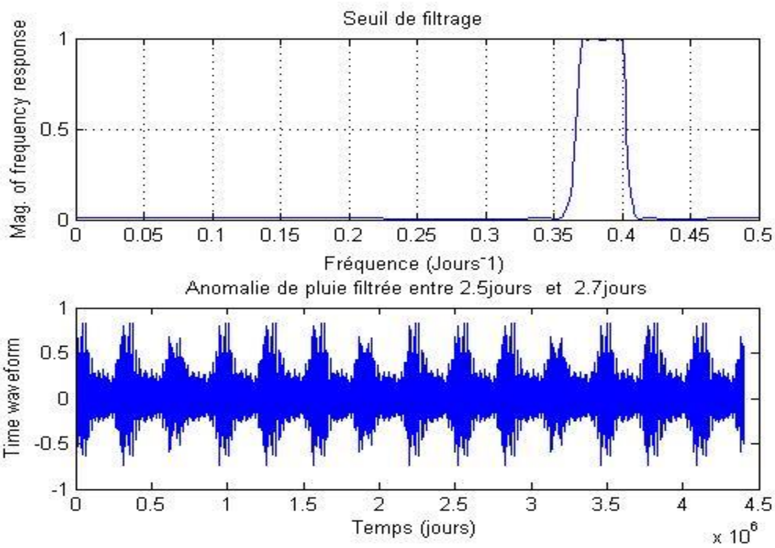

Figure 15: Filtering threshold and daily anomaly curves for filtered data between 2.5 days and 2.7 days

To determine the pseudo-periodicity of the daily rainfall anomaly, we plotted its spectral power (red colored curve) combined with the MEM. The intersections of these two curves give several points. The first intersection coordinates are defined by (X1=6.87days, Y1=0.69watts) and (X2=5.98days, Y2=0.73watts). This means that the first dominant mode of the rainfall anomaly, the first pseudo period of the signal, is X1-X2 = 0.891 days. The second intersection coordinates are defined by (X3=4.97 days, Y3=0.80watts) and (X4=3.16 days, Y4=1.27watts). This means that the second dominant mode of the rainfall anomaly, the second pseudo period of the signal, is X3-X4 = 1.81 days. And finally, the third intersection coordinates are defined by (X5=2.76 days, Y5=1.52watts) and (X6=2.49 days, Y6=1.82watts). This means that the third dominant mode of the rainfall anomaly, the third pseudo period of the signal, is X5-X6 = 0.27 days. After filtering the data of the rainfall anomaly by showing the data corresponding to the dominant pseudo period modes we quoted above. The filtering curves are shown in figures 13, 14 and 15.

4.2. Spatial analysis of rainfall over the period 1979 to 2013

4.2.1. Annual Spatial Rainfall Analysis

Analysis of annual mean values for 35 years (1979-2013) shows an inequality in the spatial distribution of rainfall in the Alaotra Mangoro region (Figure 16 below). A decrease in mean annual rainfall heights and the number of annual rainy days is observed along an East/West axis (or gradient). This spatial distribution is explained by the continentalization effect, due to the depletion of water in the precipitation-bearing air mass as it moves inland into the highlands. Linked to the presence of dense rainforest and the influence of the classical rainfall asymmetry characterizing rainfall in eastern Madagascar [18], we note the existence of a second axis of West-East growth. Indeed, at equal longitude, the eastern part of the island receives more water heights (of the order of a few hundred millimeters) than those located in the west. Two major rainfall regions can be distinguished on either side of the 2,200 mm isohyet, which generally marks the eastern limit of rainy tropical climates.

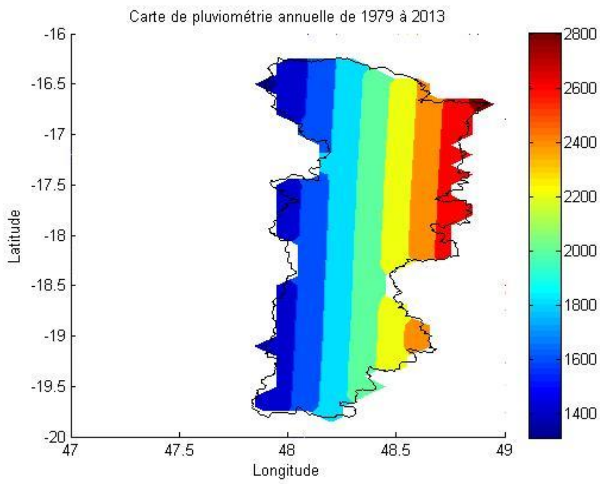

Figure 16: Map of average annual rainfall from 1979 to 2013

The total annual number of rainy days (Figure 17 below) is proportional to the annual rainfall. It is therefore maximum in the northeast corners (Andilamena) with values around 300 rainy days. The decrease in the number of rainy days from the Alaotra Mangoro region towards the interior of the country is not regular as in the case of the average annual rainfall. Spatial discontinuities are indeed encountered in some places. The decreasing rainfall gradient is in fact disturbed as we approach the district of Ambatondrazaka (center) where we note on the contrary an average increase in the annual number of rainy days, then again a continuous decrease in values after this locality towards the southwest in the districts of Moramanga and Anosibe an'Ala. These spatial peculiarities linked to local climatic conditions are also observed around the Amparafaravola district in the North-West which records less than 100 rainy days in the year while the districts of Moramanga and Anosibe an'Ala further South receive more (at least 180 rainy days). Mapping the total number of rainy days per year can in some cases overestimate the rainfall level of an area. Indeed, as long as all the rains are taken into account in the count, the number can be significant even if a non-negligible part of the rainfall barely exceeds 0.1 mm (the threshold value used by the World Meteorological Organization to record a rainy event). To give a much more realistic idea of the spatial distribution of the number of rainy days, only significant rainfall events were considered.

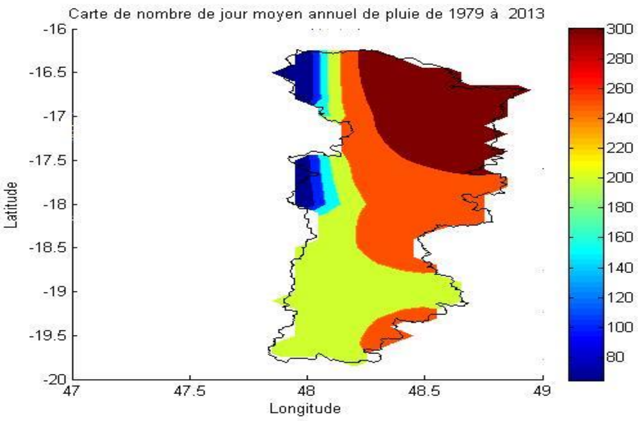

Figure 17: Map of annual number of days of rainfall from 1979 to 2013

4.2.2. Spatial Analysis of Monthly Rainfall

The spatial distribution of monthly rainfall (Figure 18 below) generally follows a decreasing northwest/southeast gradient from June to October. During this period, the heaviest rains are recorded in the southern part of the Alaotra Mangoro region. For example, during the month of June, rainfall amounts do not exceed 2.5 mm in the eastern part, while they barely reach 0.5 mm in the northwest. The same gradients are observed in March, but rainfall reaches 4 mm in the northeast. From the month of January, the gradient is reversed (increasing gradient Northeast / Northwest). The highest values are currently recorded in the Northeast. In January, for example, low rainfall is recorded in the western part of the Amparafaravola district and part of the strict Ambatondrazaka (less than 3 mm) while the maximum, a height of 4 mm, is reached in the district of Andilamena in the far north.

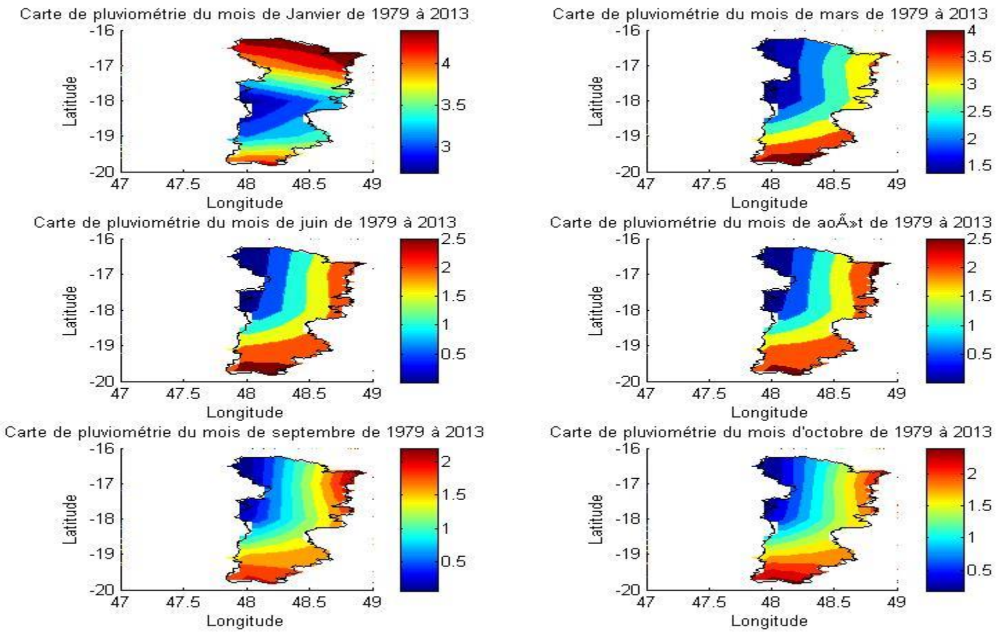

Figure 18: Map of Monthly Average Rainfall from 1979 to 2013

This spatial behavior of the monthly rainfall during the year (described above) allows for a division of the Alaotra Mangoro region into two rainfall regimes. These two regimes correspond in fact to the two-season regime, winter and summer. The monthly number of rainy days (Figure 19 below) is proportional to the annual number of days. It is therefore maximal in the northeast corners (Andilamena) with values around 25 rainy days. The decrease in the number of rainy days from the Alaotra Mangoro region towards the interior of the country does not occur on a regular basis as in the case of the annual number of days. Spatial discontinuities are indeed encountered in places in the months of June to October. The decreasing rainfall gradient is in fact disturbed as we approach the district of Ambatondrazaka (center) where we note on the contrary an average increase in the annual number of rainy days, then again a continuous decrease in values after this locality towards the southwest in the districts of Moramanga and Anosibe an'Ala in the months of September and October. We note the same number of monthly rainy days in this part in the months of June and August. These spatial peculiarities linked to local climatic conditions are also observed around the district of Amparafaravola in the North-West which records less than 5 rainy days during the month of June to September while the districts of Moramanga and Anosibe an'Ala further South receive more (at least 20 rainy days in the month of June to August and at least 15 days in the month of September to October).

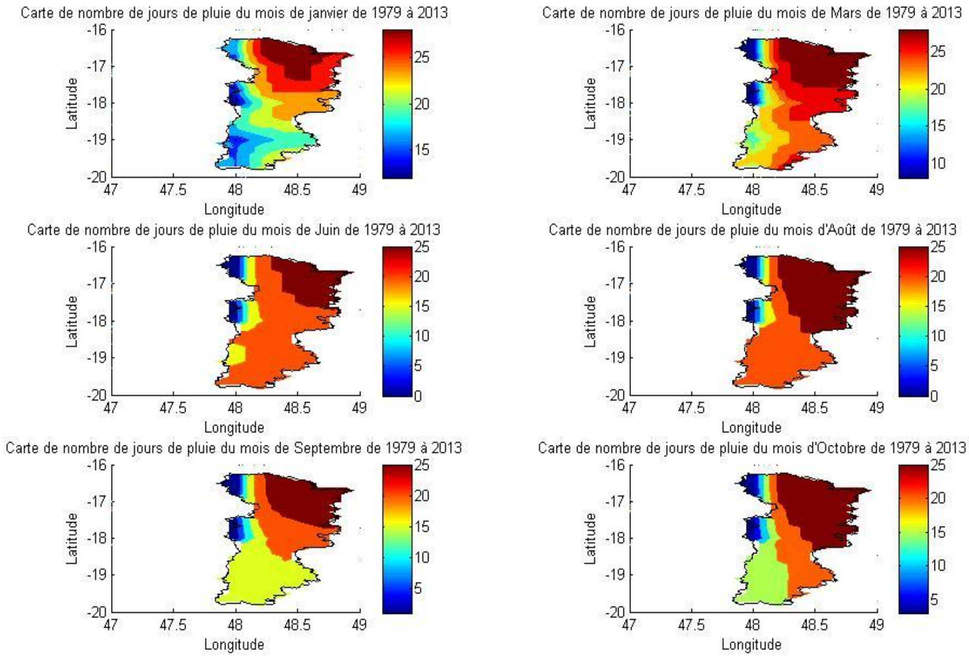

Figure 19: Map of Number of Monthly Rainfall Days from 1979 to 2013

We see the opposite case in January and March, i.e. the number of rainy days per month shows a decreasing rainfall gradient from North-East to South-West. The number of rainy days reaches the maximum, up to 25 rainy days in the Northeast part while it reaches only 10 days in the Southeast part of the region.

4.2.3. Spatial analysis of rainfall over the decades 1979-1988, 1989-1998, 199-2008

During these three decades, annual rainfall has declined remarkably (see figure 20). Indeed, the maps in Figure 21 (below) describe the evolution of rainfall during these three decades. Classes delimited by the isohyets 1 200 mm and 2 400 mm are observed for the first decade (1979 - 1988), between 700 mm and 1 500 mm for the second (1989 - 1998) and between 600 mm and 1 100 mm for the third (1999 - 2008). Rainfall has a tendency to decrease by up to half for the last two decades. In addition, as the interannual rainfall for 35 years (see Figure 16), we note a decrease in the average annual rainfall is observed, along an East/West axis (or gradient). Then, we also observe that this gradient becomes more and more amplified during the last two decades 1989 - 1998 and 1999 - 2008. The decade 1979 - 1988 is quite rainy. The Alaotra Mangoro region is limited by the isohyets curves 2,400 mm on the extreme East, between 2,000m and 2,200 m for the Middle East and between 1,600 mm and 1,800 mm in the Centre. The other western regions receive less, i.e. rainfall between 1,200 mm and 1,400 mm. During the decade 1989-1998, the decline in rainfall took on particular importance in the Alaotra Mangoro region. This decrease concerns almost the entire region. The zone of rainfall below 1,500 mm widens sharply and occupies almost the entire region. We observe the decrease in rainfall almost half compared to the previous decade. This shift towards the Center of the 1500 mm isohyet is accompanied by the appearance of a zone of rainfall below 1000 mm in the Center towards the West (threshold value that indicates the transition from a humid tropical climate to a dry tropical climate). This means that the climate of the region is divided in two in the center during the decade 1989- 1998. The climate from the center to the east is characterized by a humid tropical climate while from the center to the west is characterized by a dry tropical climate.

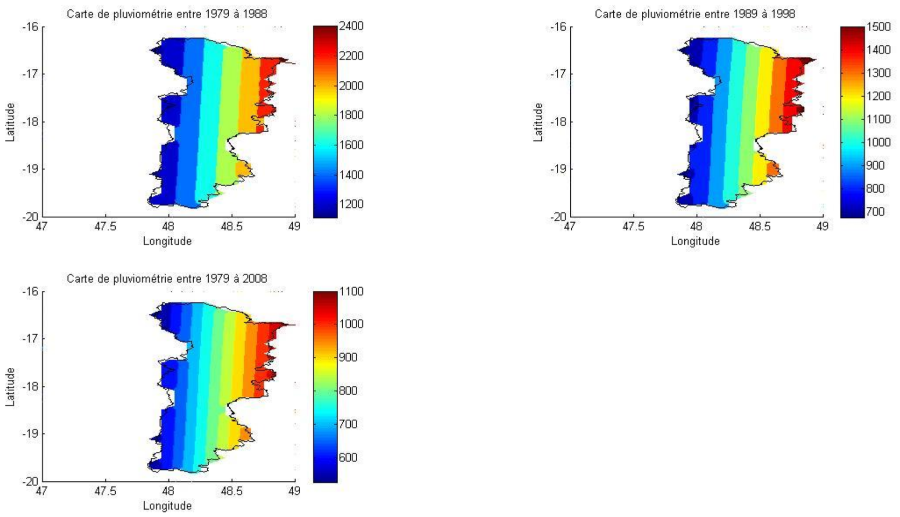

Figure 20: Map of average rainfall over the decades 1979-1988, 1989-1998, 1999-2008

This decrease in rainfall is accentuated during the decade 1999-2008. The zone of rainfall below 1,000 mm widens over almost the entire region and during this period it advances eastward. Only a small part of the region in the far east records a rainfall of 1,100 mm. This allows us to say that the climate of the Alaotra Mangoro region over the last decade is moving towards a dry tropical climate.

4.2.4. Spatial analysis of rainfall during the quinquas from 1979 to 2013

In this analysis, we try to see the details of the change in precipitation in five-year increments over the period 1979 to 2013 (see Figure 21). The decrease in rainfall is of colossal importance in the Alaotra Mangoro region. This decrease concerns almost the entire region and particularly during the last five-year period, 2008 to 2013, with a rainfall value that drops to 350 mm. After the first five years, from 1979 to 1983 with a precipitation value of 2,400 mm, the decrease in this amount is very remarkable. During the periods 1984-1988 and 1994-1998 the amount of rainfall does not exceed the value of 1,100 mm. While during the other quinquenas, this amount of precipitation does not exceed 600 mm. A remarkable decrease is observed between 2008 and 2013. The amount of precipitation does not exceed the value of 350 mm. This indicates that the climate trend in the Alaotra Mangoro region tends towards dry tropical climate. This indicates that climate change in terms of precipitation is very present in this region.

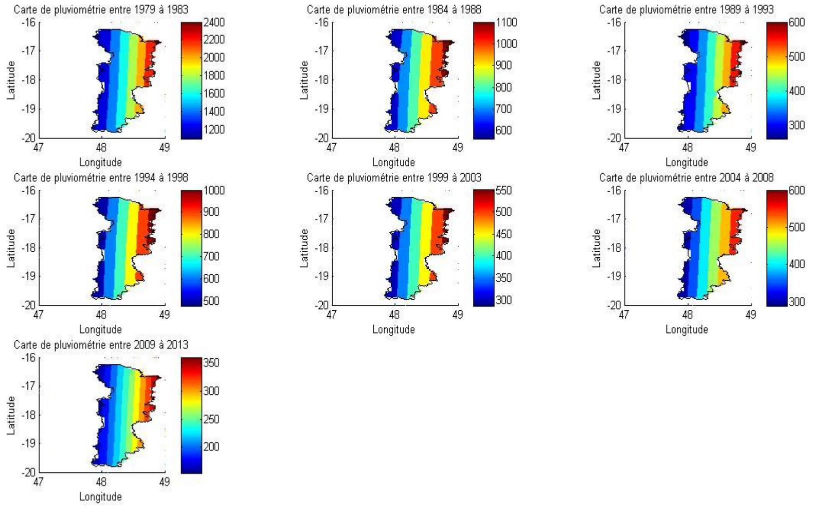

Figure 21: Map of average precipitation during the quinquas from 1979 to 2013

4.2.5. Spatial analysis of rainfall by the Principal Component Analysis method

Using the Principal Component Analysis (PCA) method, we will study the spatial distribution of monthly rainfall in the Alaotra Mangoro region from January to December over the period 1979 to 2013. First, the rainfall data for the Alaotra Mangoro region will be reorganized in a table. The months are placed in columns and the dots are in rows. The months are the variables to be explained while the points, having longitude and latitude coordinates, will be used as individuals. The study area is divided into several grids, each containing an individual. The months with the most rainfall are the first three months of the year: January, February and March with an average of more than 2.5 mm. While September is the driest month with an average of 0.95 mm (~1 mm). The mean and standard deviation are given in Table 1.

Table 1: Mean and Standard Deviation

	Moyenne (mm)	Ecartype
Janvier	3,66	0,56
Février	3,94	0,41
Mars	2,53	1,01
Avril	1,44	1,08
Mai	1,38	1,15
Juin	1,19	1,01
Juillet	1,29	1,09
Août	1,17	0,98
Septembre	0,95	0,76
Octobre	1,11	0,77
Novembre	1,33	0,66
Décembre	2,11	0,59

The correlation matrix between the months of the year is given in Table 2. In Table 2, we see that all months are positively correlated with each other. We will characterize the rainfall correlation relationships over the 35 years between the months. The above table shows us three types of correlation. A very strong correlation for a value very close to 1, a strong correlation for a value between 0.5 and 1, and a weak correlation for a value between 0 and 0.5.

Table 2: Correlation Matrix between Variables

	Janvier	Février	Mars	Avril	Mai	Juin	Juillet	Août	Septembre	Octobre	Novembre	Décembre
Janvier	1,00	0,89	0,36	0,33	0,27	0,31	0,30	0,31	0,35	0,34	0,40	0,62
Février	0,89	1,00	0,55	0,55	0,51	0,56	0,56	0,57	0,60	0,58	0,62	0,73
Mars	0,36	0,55	1,00	0,99	0,99	0,97	0,96	0,96	0,94	0,97	0,97	0,91
Avril	0,33	0,55	0,99	1,00	0,99	0,99	0,98	0,98	0,97	0,99	0,98	0,89
Mai	0,27	0,51	0,99	0,99	1,00	0,98	0,97	0,96	0,95	0,98	0,98	0,88
Juin	0,31	0,56	0,97	0,99	0,98	1,00	1,00	1,00	0,99	1,00	0,97	0,86
Juillet	0,30	0,56	0,96	0,98	0,97	1,00	1,00	1,00	0,99	1,00	0,97	0,85
Août	0,31	0,57	0,96	0,98	0,96	1,00	1,00	1,00	1,00	1,00	0,96	0,85
Septembre	0,35	0,60	0,94	0,97	0,95	0,99	0,99	1,00	1,00	0,99	0,96	0,85
Octobre	0,34	0,58	0,97	0,99	0,98	1,00	1,00	1,00	0,99	1,00	0,98	0,89
Novembre	0,40	0,62	0,97	0,98	0,98	0,97	0,97	0,96	0,96	0,98	1,00	0,93
Décembre	0,62	0,73	0,91	0,89	0,88	0,86	0,85	0,85	0,85	0,89	0,93	1,00

By analyzing the table representing the correlation matrix between the months, we find a correlation between the months of the dry season, between the months of the rainy season and between the months of these two seasons. We observe a very strong correlation of rainfall during the dry season, i.e. between the months of June, July, August and September. In the same way this type of correlation is valid between the months of June, July, August and October. We also observe a very strong correlation of rainfall during the rainy season, that is, between the months of January and February, March and April. Finally, we observe a very strong correlation of rainfall between the two seasons. The month of December is an exception because the rainfall of all the months during the year has a very strong and/or strong correlation with this month. We see the same observation for the month of November with the exception of the month of January. From the above correlation matrix, we can say that for the Alaotra Mangoro region, rainfall during the wet season has a strong correlation with rainfall during the dry season. Table 3 above shows the eigenvalues, the percentages of variances and the percentages of their accumulation.

Table 3: Eigenvalues, percentages of variances and their accumulation

Valeur propre	Variance (%)	Variance cumulée (%)
10,197	84,973	84,973
1,479	12,326	97,298
0,200	1,665	98,963
0,059	0,495	99,458
0,046	0,382	99,840
0,011	0,092	99,932
0,005	0,038	99,970
0,003	0,025	99,994
0,000	0,004	99,998
0,000	0,001	99,999
0,000	0,000	100,000
0,000	0,000	100,000

Figure 22 below shows the curves representing the histogram and the eigenvalue curve, the curve of the percentages of the cumulative variances.

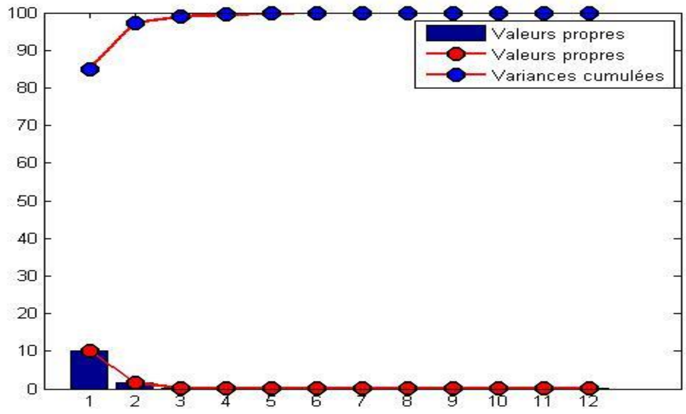

Figure 22: Curve of Eigenvalues and Cumulative Variances

To have more information by reducing the number of variables, let us retain the first two axes, 1 and 2, which retain the 96.291% of the information or initial inertia. We retain these two main axes for the following because according to Kaiser's criterion, the eigenvalues corresponding to them are greater than or equal to 1. In addition, the "elbow" rule adds that we cut the scree from the eigenvalues at the place where it has a "elbow". The correlation circles and the representations of individuals on the first two main axes are shown in figures 23 and 24 respectively. Axis 1 represents the amount of rainfall during the month of October. This is the dry period in the Alaotra Mangoro region. The strong positive correlation of this variable, October, with the first main axis 1 is the explanation. The shift to the left explains the decrease in the amount of rainfall during the month of October. The second axis 2 represents the opposite of the first, the amount of rain during the month of January. That is, during the rainy period in the region. This axis therefore allows to classify in its positive part the areas with a significant amount of rain that will decrease when the movement goes down or to its negative side.

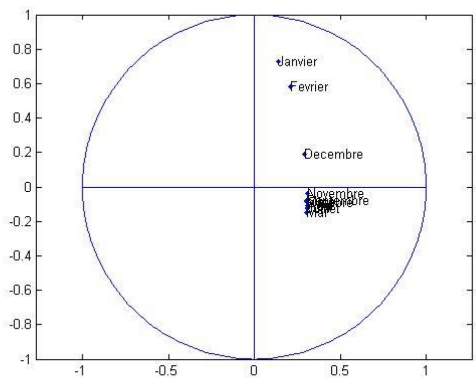

Figure 23: Correlation Circle of Variables

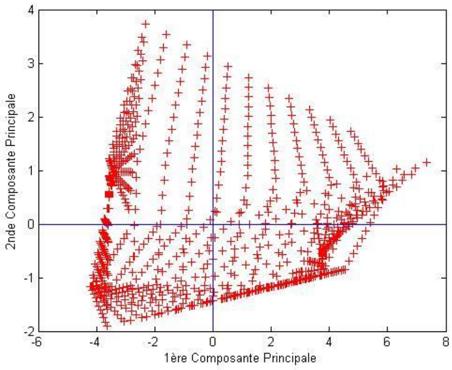

Figure 24: Representation of individuals on the main axes

The cartographic representations of the individuals on the two main axes are shown in figures 25 and 26 respectively. The values in brown (figures 25, 26) are the coefficients of the good presentation of the individuals on the two main axes 1 and 2. During the month of October the distribution of rainfall in the Alaotra Mangoro region, represented by the above map, is explained by :

The existence of homogeneous groupings of individuals in blue with very low rainfall or almost dry; The grouping of small areas in green and yellow because of their low rainfall; The increase in the amount of rainfall observed moving towards the eastern part of the region. Indeed, the grouping of several areas colored in brown in the eastern part of the study area, shows the existence of heavy rainfall in the eastern part of the region. The presence of an average amount of rain in the area formed by the orange colored zone. The eastern part of the Alaotra Mangoro region is the wettest during the month of October. While, the quantity of rain decreases and the area becomes almost dry like the western part of our study area. During the rainy season, two regions with homogeneous rainfall amounts were observed:

The existence of homogenous blue groupings of individuals with very low rainfall or near-dry conditions is found in the central part of the region; The increase in the amount of rainfall observed moving towards the northwestern part of the region. Indeed, the grouping of several brown-coloured areas in the northwestern part of the study area indicates the existence of heavy rainfall in this part.The presence of an average amount of rain in the area formed by the orange colored zone.

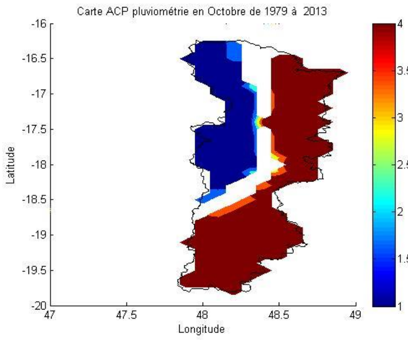

Figure 25: Rainfall distribution map on the first main axis

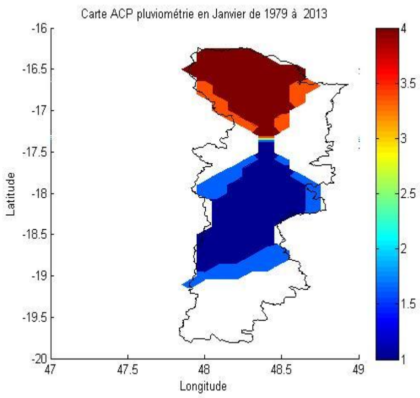

Figure 26: Rainfall distribution map on the second main axis

5. Conclusion and Perspectives

The rainfall data processing chains thus perform several functions on raw data loading, data correction, reconstruction of missing values, calculation of averages over various time periods, spectral analysis of anomalies, calculation of grids of values and area averages, cartographic representation of results in the form of isovaleurs or draped contour plots and spatial analysis in principal components. This chain constitutes an operational tool adapted to the processing and visualization of rainfall data commonly used in climatology and will evolve according to the needs of climate scientists and new data. In the case of the calculation of averages in time and space, the time saving is considerable, since it took only a few minutes to perform all the operations described above in a region and, in particular, to calculate the average annual rainfall in the Alaotra Mangoro region for 35 years. The values obtained manually are very similar to those obtained automatically by these processing lines. In general it would seem that the best results are obtained by choosing an interpolation step as close as possible to the actual density of the observation area. These processing chains can be applied not only in other regions of Madagascar but also for the spatio-temporal analysis of other climatic parameters such as temperature, wind speed, air humidity and specific humidity, etc. A generalization of modeling and formalization of processing chains will be proposed for the continuation of our research in order to take into account large volumes of data, the interoperability of these chains through existing spatial data information systems in the field of climatology at the regional and/or global level.

References

[1]. http://www.blftrade.com/fr/trouver-un-marche/fiches-pays/madagascar/economie-3 (consulted on 14-08-2014)

[2]. Ratsivalaka A. S., 2011. Quelques techniques de la télédétection appliquées à Madagascar à l'étude des changements climatiques et leurs impacts sur l'environnement. Madagascar-Revue de Géographie, volume 48 Page 12, Juillet 2011- Décembre 2011

[3]. Razakavololona A., 2011. Indicateurs de vulnérabilité des exploitations agricoles face aux variabilités climatique et démographique: applications a la riziculture dans la région du lac Alaotra (Madagascar). Thèse de doctorat, Ecole Supérieure des Sciences Agronomiques, Université d'Antananarivo, octobre

2011.

[4]. Shukri A. et Mustapha D., 2013. Mission FAO/PAM d'évaluation de la sécurité alimentaire à Madagascar. juin 2013.

[5]. Dakhmouche M., 2010. Introduction à la Statistique Descriptive. Ecole Préparatoire en Sciences Economiques Commerciales Et des Sciences de Gestion de Constantine, Algérie, pp. 98.

[6]. Burg J. P., 1967. Maximum entropy spectral analysis. in Proc. of the 37th Meeting of the Society of Exploration Geophysicists, (Oklahoma City), pp. 34–41, October 1967.

[7]. Picinbono B. et Barret M., 1990. Nouvelle présentation de la méthode du maximum d'entropie. Laboratoire des Signaux et Systèmes, ESE, Plateau de Moulon, Technopole de Metz, vol.7(2), France

[8]. Press W. H., Teukolsky S. A., Vetterling W. T, Flannery B. P., 1992. Numerical Recipes in C. Cambridge university press vol.2.

[9]. Labarriere M., Krief J.-P., Gimonet B., 1993. Le filtrage et ses applications, Cepadues Edition.

[10]. Jolliffe I. T., 2002. Principal Component Analysis. Second ed. Springer. Series in Statistics. New York: Springer-Verlag New York. PEARSON, Karl, 1901.

[11]. Ambapour S., 2003. Introduction à l'analyse des données. Bureau d'Application des Méthodes Statistiques et Informatiques, Brazzaville, avril 2003.

[12]. Saporta G., 2006. Probabilités, analyse des données et statistique. 2e édition révisée et augmentée, Paris : Editions Technip, France.

[13]. Delmas J-F. et Salam S., 2009. Analyse en composantes principales. SCILAB à l'Ecole des Ponts ParisTech (http://cermics.enpc.fr/scilab_new/site/Tp/Statistique/acp/index.htm) (Consulté le 18/01/2015).

[14]. Richard Goering, 2004. Matlab edges closer to electronic design automation world. EE Times

[15]. The MathWorks, 2003. Statistics Toolbox User's Guide Version 4.1. Revised for Version 4.1 (Release 13.0.1)

[16]. The MathWorks, 2001. Signal Processing Toolbox User's Guide. Revised for Version 5.1 (Release 12.1)

[17]. The MathWorks, 2009. Mapping Toolbox™ User's Guide. Revised for Version 3.0 (Release 2009b)

[18]. Gerald D., 1971. Contribution géographique à l'étude du climat de Madagascar.